"Structure and Assembly of the SF3a Splicing Factor Complex of U2 snRNP"
Pei-Chun Lin & Rui-Ming Xu

Supplementary information

Figure S1. Electron density maps. (A) A section of the initial 3.5 Å SeMet MAD phased electron density map contoured at 1.5 σ. The positions of Se atoms used for phasing are indicated with magenta spheres. The Cα trace of the refined model is superimposed for reference. (B) Stereo view of a section of the 3.1 Å 2Fo-Fc electron density map. The map is contoured above 2.0 σ, and a refined model of the SF3a core is superimposed.

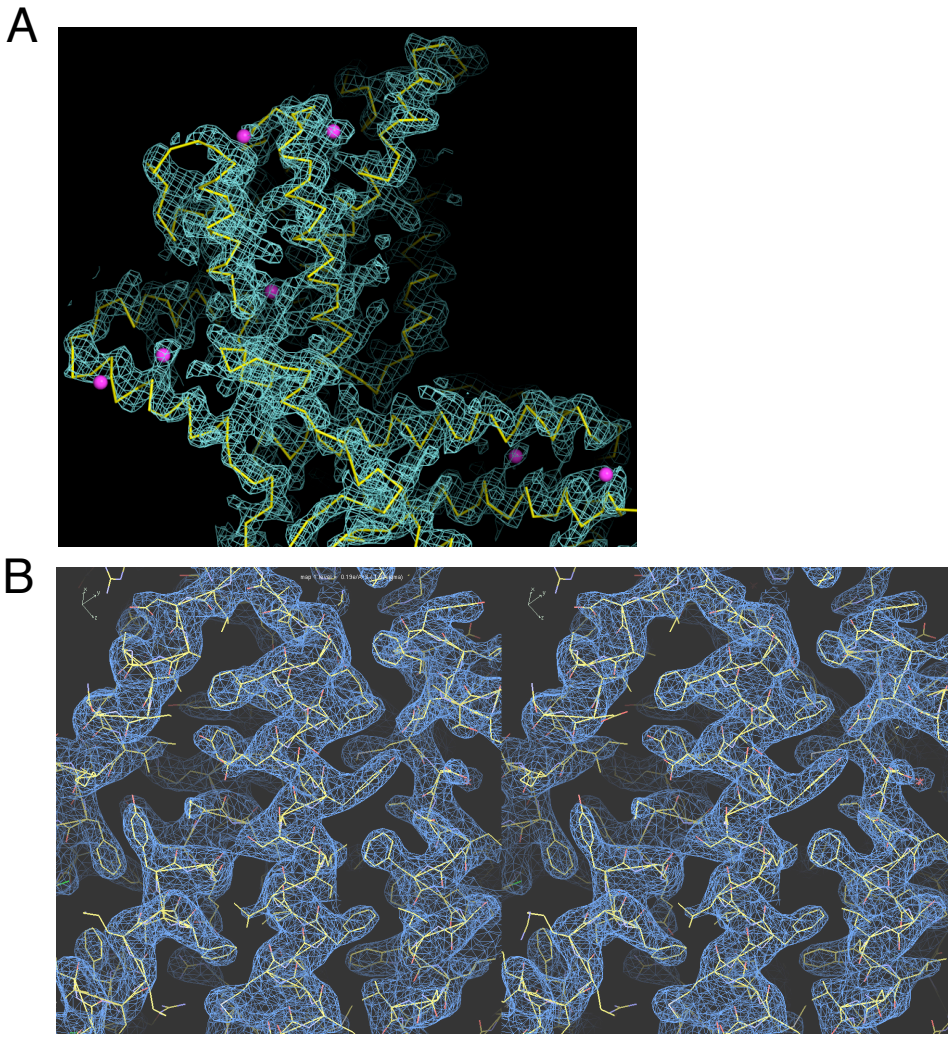

Figure S2. Structure determination of Prp11ΔN. (A) SeMet anomalous difference peaks of six Prp11ΔN point mutants (L153M, A174M, V183M, V200M, V252M) were used for assignment of sidechains. These mutated residues are shown in a stick model (colored magenta) superimposed onto a ribbon representation of Prp11ΔN. The sidechains of a 36-residue N-terminal fragment cannot unambiguously assigned, and these 36 residues are represented in a polyalanine model colored in yellow. (B) SDS-PAGE analysis shows no sign of protein degradation of the crystallized SF3a components.

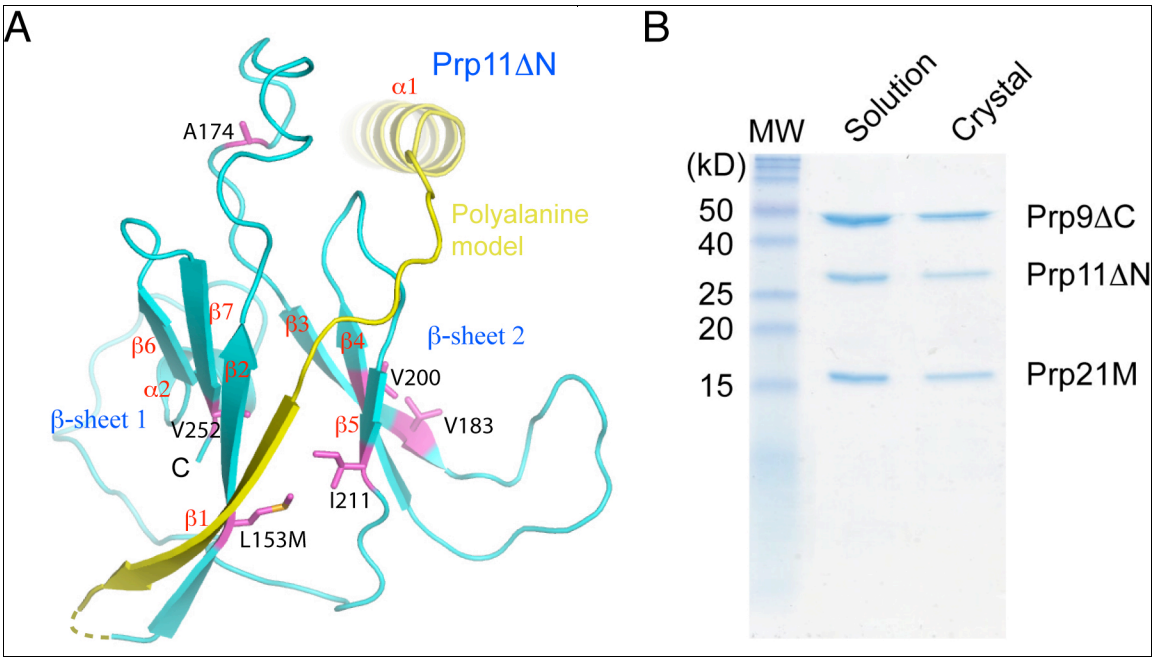

Figure S3. Binding of the full-length and the SF3a core complexes to synthetic yeast U2 snRNA fragments detected using EMSA. SL1, SL2a, SL2b, and SL4 indicate stem-loops I, IIa, IIb, and IV, respectively, and BPRS denotes the branch point recognition sequence of U2 snRNA.

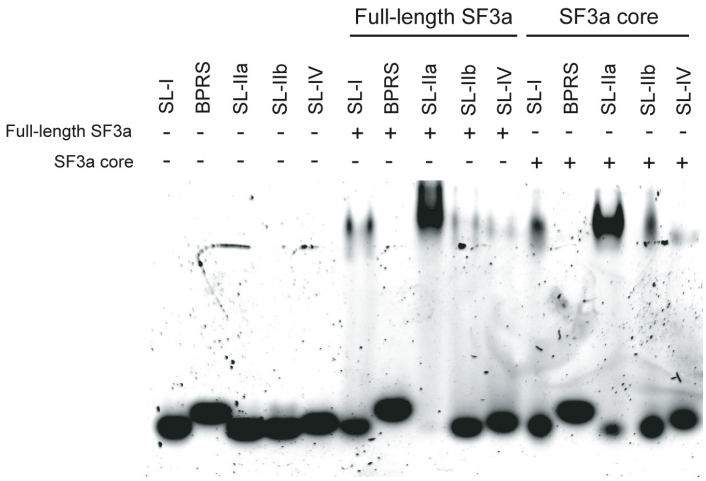

Figure S4. RNA binding properties of Prp9 mutants. (A) Location of positively charged residues mutated in the Prp9 triple (K302E, K305E & K306E) and double (R114E & K115E) mutants. The SF3a core complex is shown in a surface representation with surface electrostatic potential distribution (blue: positively charged; red: negatively charged). (B) EMSA results of the wild-type (WT), the triple and double mutants of the SF3a core complex with various fragments of yeast U2 snRNA. Please note that the triple mutation of residues near the zinc finger at the CTD of Prp9 interferes with SL2a binding, while the double mutation (R114E & K115E) at the NTD has little effect on SL2a binding. (C) The Prp9-21N complex, composed of Prp9ΔC and the N-terminal half (a.a. 87-176) of Prp21M, binds to SL2a, while the Prp11-21C complex, composed of Prp11ΔN and the C-terminal half (a.a. 177-237) of Prp21M, does not bind U2 snRNA. The mixture of Prp9-21N and Prp11-21C appears to reduce the non-specific binding of Prp9-21N to SL1.

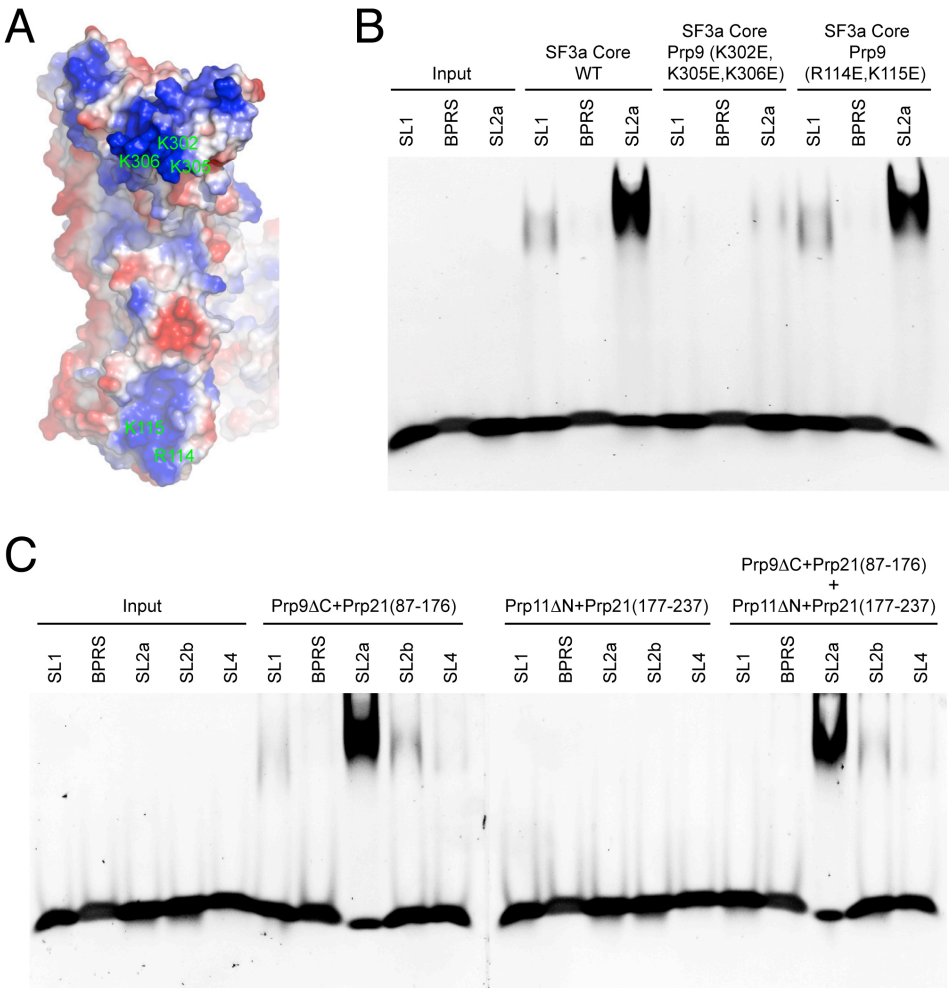

Figure S5. Alignment of amino acid sequences of yeast Prp9 and human SF3a60. An asterisk, a colon and a period at the bottom of the sequence indicate identical, highly similar and similar residues between the yeast and human proteins, respectively. A schematic representation of the Prp9 secondary structure is shown above the sequence, and the secondary structural elements of the N- and C-terminal domain are labeled with white and black letters, respectively.